Escape of particles in a time-dependent potential well

Diogo Ricardo da Costa,[1] Carl P. Dettmann,[2] and Edson D. Leonel[1]

[1]*Departamento de Estatística, Matemática Aplicada e Computação, UNESP—Universidade Estadual Paulista,
Avenida 24A, 1515 CEP 13506-900, Rio Claro, São Paulo, Brazil*
[2]*School of Mathematics, University of Bristol, Bristol, United Kingdom*

We investigate the escape of an ensemble of noninteracting particles inside an infinite potential box that contains a time-dependent potential well. The dynamics of each particle is described by a two-dimensional nonlinear area-preserving mapping for the variables energy and time, leading to a mixed phase space. The chaotic sea in the phase space surrounds periodic islands and is limited by a set of invariant spanning curves. When a hole is introduced in the energy axis, the histogram of frequency for the escape of particles, which we observe to be scaling invariant, grows rapidly until it reaches a maximum and then decreases toward zero at sufficiently long times. A plot of the survival probability of a particle in the dynamics as function of time is observed to be exponential for short times, reaching a crossover time and turning to a slower-decay regime, due to sticky regions observed in the phase space.

I. INTRODUCTION

After the seminal result of Buttiker and Landauer [1] on tunneling through a time-dependent potential barrier, interest in the dynamics of a particle in a driven potential has markedly increased. This dynamics can be described using both theoretical and experimental approaches and can be considered using either classical or quantum characterization. Several applications have been discussed, including ballistic conductance in a periodically modulated channel [2], magnetotransport through heterostructures of GaAs/AlGaAs [3], sequential resonant tunneling in semiconductor superlattices due to intense electrical fields [4], influence of transport in the presence of microwaves [5], anomalous transmission in periodic waveguides [6], trapping in driven barriers [7], characterization of traversal time [8,9], symmetry breaking and drift of particles in a chain of potential barriers [10], Lyapunov characterization of chaotic dynamics and destruction of invariant tori [11], among many others [12,13].

The classical case of a time-dependent one-dimensional potential is a $1\frac{1}{2}$-degree-of-freedom problem. The most common formalism used is the so-called mapping description. The phase space exhibits a very intricate mixed structure typical of area-preserving dynamics, including a set of islands surrounded by a chaotic sea that is confined by a set of invariant tori (also called invariant spanning curves). In many cases, the chaotic dynamics of the particle inside the driven potential leads to very interesting phenomena, including power law distribution for the trapping [14], scattering [15], and critical exponents for the average properties of the chaotic sea [16]. It was also shown that an external periodic field changes the asymptotic populations of the asymmetric energy levels [17] and a stochastic perturbation can lead the particle to experience unlimited energy growth [18].

The mixed form of the phase space leads to nonuniformity [19] and sticky domains [20] that produce anomalous transport. A sticky region *traps* a particle in the phase space and the escape from this region happens at a very long time after the entrance. This part of the orbit is relatively regular and, since the particle spends more time in such a sticky

zone than elsewhere, important observables like recurrence times [21] and Lyapunov exponents [22] are directly affected. Stickiness may be quantified in terms of the distribution of recurrence times of a typical orbit in the phase space. For fully chaotic dynamics, the decay is exponential [23], while for mixed phase space it is observed to be described approximately by a power law [24]. This power law arises from combined effects of an infinite hierarchy of islands with a corresponding hierarchy of time scales. Recent investigations of resonance splittings and homoclinic tangles in the vicinity of islands may provide insight into these mechanisms [25–28].

Recurrence statistics are also intimately related to the statistics of escape from a region containing an initial distribution of particles into a *hole*, where again exponential or power law decay can be observed for fully chaotic or mixed dynamics, respectively [29]. These statistics also provide useful information for the control of chaotic systems [30]. Escape properties measured as a function of a varying hole provide a further sensitive and nondestructive probe of the dynamics [31]. Very recently this approach has also been successfully applied to a time-dependent Hamiltonian system [32].

In this paper we consider the dynamics of a classical particle confined inside an infinite potential box which contains an oscillating square well, with the aim of understanding the escape of particles to a defined hole in the energy coordinate. The Hamiltonian that describes the model is $H(x,p,t) = p^2/(2m) + V(x,t)$, where $V(x,t) = V_0(x) + V_1(x,t)$, and x, p, and t correspond to the position and momentum coordinates and the time, respectively. The potential $V_0(x)$ denotes the integrable part of the Hamiltonian while $V_1(x,t)$ leads to the nonintegrable part. As we will see in the next section, the potential $V_1(x,t)$ is controlled by three relevant control parameters. If the amplitude of oscillation of the moving well is fixed to zero, the system is integrable and the phase space exhibits only regular dynamics. On the other hand, if $V_1(x,t) \neq 0$, the phase space becomes mixed thus exhibiting islands, chaotic seas, and invariant spanning curves.
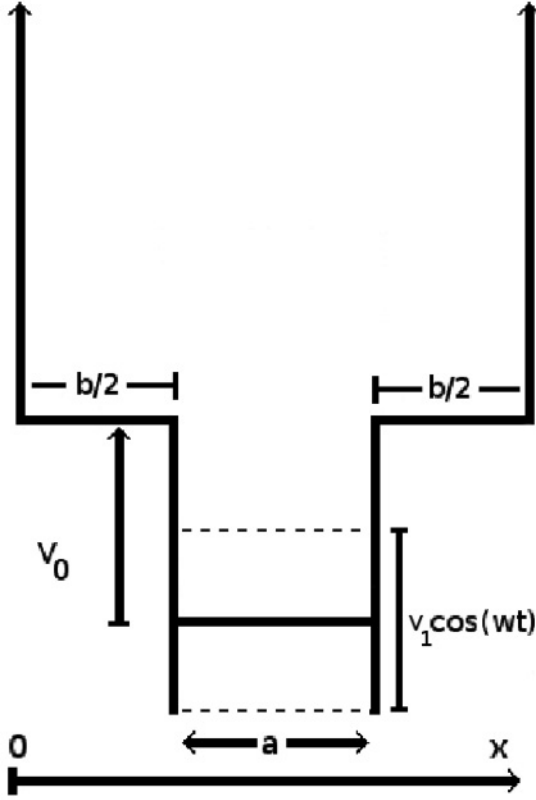
FIG. 1. Sketch of the potential.

Depending on the region of the phase space considered, one can observe fully chaotic dynamics leading to an exponential distribution of the recurrence time. However, when islands are present, they produce an approximately power law decay due to the stickiness.

This paper is organized as follows: In Sec. II we describe the model and the map. The numerical results and discussions are also presented in this section. Final conclusions are drawn in Sec. III.

II. THE MODEL, THE MAP, AND NUMERICAL RESULTS

We have considered the dynamics of a classical particle confined inside a box of infinite potential which contains a periodically oscillating square well in the middle. A typical sketch of the potential is shown in Fig. 1.

The potential $V(x,t)$ is given by

$$V(x,t)$$
$$= \begin{cases} \infty & \text{if} \quad x \leqslant 0 \text{ or } x \geqslant (a+b), \\ V_0 & \text{if} \quad 0 < x < \frac{b}{2} \text{ or } (a+\frac{b}{2}) < x \\ & \quad < (a+b), \\ V_1 \cos(\omega t) & \text{if} \quad \frac{b}{2} \leqslant x \leqslant (a+\frac{b}{2}), \end{cases} \quad (1)$$

where the control parameters a, b, V_0, V_1, and ω are constants. Given the symmetry of the problem, we update the variables of the two-dimensional mapping at each entrance of the particle into the oscillating square well. A step by step derivation of the equations of the mapping can be obtained in Ref. [16]. It is appropriate to define dimensionless variables $\delta = V_1/V_0$,
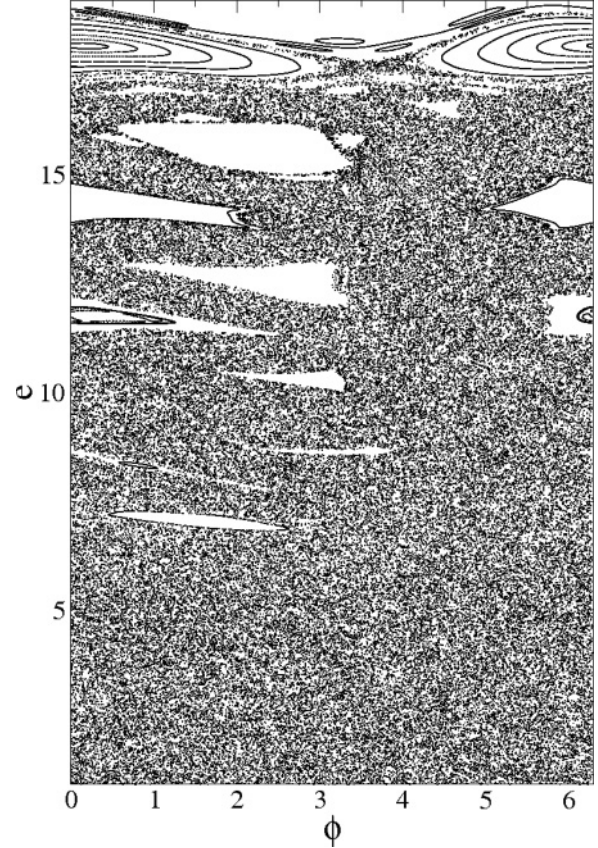
FIG. 2. Phase space for the map (2). The control parameters used were $r = 1$, $\delta = 0.5$, and $N_c = 33.18$.

$r = b/a$, $e_n = E_n/V_0$, and $N_c = \omega/(2\pi)(a/\sqrt{2V_0/m})$ and measure the time in terms of the number of oscillations of the moving well, $\phi = \omega t$. Here N_c corresponds to the number of oscillations that the square well completes in a time $t = a/\sqrt{2V_0/m}$. Given that N_c is proportional to ω, changing N_c implies changing the driving frequency ω. The mapping is written as

$$T : \begin{cases} e_{n+1} = e_n + \delta(\cos(\phi_n + i\Delta\phi_a) - \cos\phi_n), \\ \phi_{n+1} = [\phi_n + i\Delta\phi_a + \Delta\phi_b]\text{mod}2\pi, \end{cases} \quad (2)$$

where the auxiliary variables are given by

$$\Delta\phi_a = \frac{2\pi N_c}{\sqrt{e_n - \delta\cos(\phi_n)}}, \quad \Delta\phi_b = \frac{2\pi N_c r}{\sqrt{e_{n+1} - 1}},$$

where i is the smallest integer number which makes the relation $[e_n + \delta(\cos(\phi_n + i\Delta\phi_a) - \cos(\phi_n))] > 1$ true.

The determinant of the Jacobian matrix is equal to unity and the mapping (2) is area preserving. The phase space is mixed and contains periodic islands, a large chaotic sea, and a set of invariant spanning curves that prevent the particle from gaining unlimited energy from the moving well. Figure 2 shows a typical plot of the phase space for the control parameters $r = 1$, $\delta = 0.5$, and $N_c = 33.18$, which corresponds to a moderate frequency of oscillation (see Ref. [15] for specific details). We must emphasize that an initial condition in the chaotic sea cannot penetrate the island nor cross the invariant spanning curve.
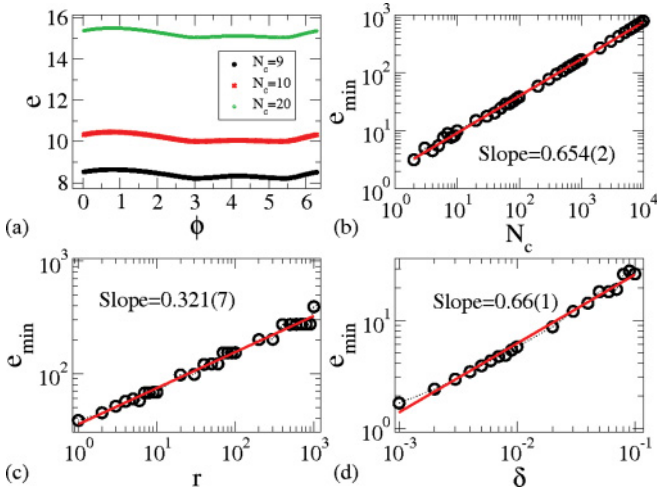
FIG. 3. (Color online) (a) Position of the lowest-energy invariant spanning curves for the driving frequency parameter N_c values 9, 10, and 20, using $r = 1$ and $\delta = 0.5$. (b) Plot of e_{min} vs N_c for $r = 1$ and $\delta = 0.5$. (c) Plot of e_{min} vs r for $N_c = 99.54$ and $\delta = 0.5$. (d) Plot of e_{min} vs r for $N_c = 99.54$ and $r = 1$.

Our numerical results will be obtained as a function of the three control parameters N_c, δ, and r as well as the number of iterations, n. Let us start with the parameter N_c. As it increases, the auxiliary variables $\Delta\phi_a$ and $\Delta\phi_b$, which depend linearly on N_c, increase too. Such a growth reduces the correlation between ϕ_{n+1} and ϕ_n, causing the phase space location of the lowest-energy invariant spanning curve to rise. For example, the curves for the control parameters $N_c = 9$, 10, and 20 for fixed $r = 1$ and $\delta = 0.5$ are shown in Fig. 3(a). A plot of the minimum energy along the invariant spanning curve as a function of N_c is shown in Fig. 3(b). A power law fitting gives $e_{min} \propto N_c^{\alpha_1}$, where $\alpha_1 = 0.654(2)$. We stress that α_1 is closely related to the critical exponent obtained in [33]. Extensions for the other control parameters can also be made as shown in Fig. 3(c) for r, leading to $e_{min} \propto r^{\alpha_2}$ with $\alpha_2 \cong 0.321(7)$ and Fig. 3(d) for δ yielding $e_{min} \propto \delta^{\alpha_3}$ with $\alpha_3 \cong 0.66(1)$. Grouping the three control parameters in a single expression, we obtain $e_{min} \propto N_c^{\alpha_1} r^{\alpha_2} \delta^{\alpha_3}$.

Let us now introduce a energy window through which the particle can escape. Specifically, the particle escapes from the potential when its energy increases beyond a given critical value. We define this critical energy as a fraction of the lowest energy among the invariant spanning curves, as for example $h = 0.7e_{min}$ (other values were also used). Then, we start an ensemble of 10^7 particles with low energy, say $e_0 = 1.01$, and 10^7 different initial phases $\phi_0 \in [0, 2\pi)$, and let them evolve in time (as we discuss below, other values of initial energy were used too). If, along the orbit, the particle reaches the critical level, we determine that the particle escapes from the potential and a new initial condition is chosen. A histogram of the distribution of escape times (rescaled to 1 for visual purposes) is shown in Fig. 4(a). We see that very few particles escape at very short times. The escape rate increases rapidly and reaches a peak, marking a preferred iteration number, which we denote as n_p, and then decreases again, approaching zero asymptotically. When the initial energy is raised, say $e_0 = 2$, $e_0 = 3$, and so on, the number of iterations needed for the
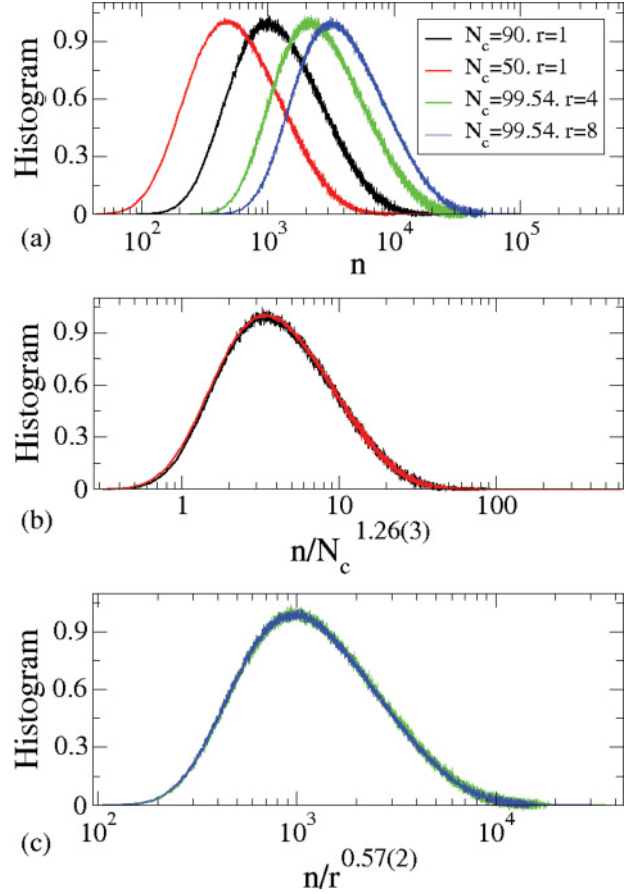

FIG. 4. (Color online) (a) Histogram of the frequency of escape as a function of the number of iterations for different control parameters. (b) Overlap of different histograms obtained for fixed r and δ and varying N_c. (c) Overlap of different histograms obtained for fixed N_c and δ and varying r.

particle to reach the escape hole decreases as long as the initial energy increases. To illustrate this behavior, Fig. 5 shows three plots of n_p vs e_0. One sees that, as the initial energy increases, the particle needs fewer iterations to reach the hole, therefore leading to a decrease in n_p. Our simulations, however, were inconclusive regarding the variation of the parameter δ, as
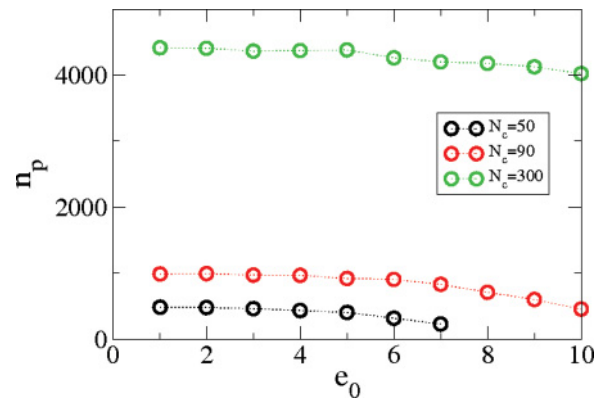

FIG. 5. (Color online) Plot of n_p vs e_0. One sees clearly that as long as the energy increases, n_p decreases. The control parameters used were $r = 1$ and $\delta = 0.5$ while N_c is labeled in the figure.
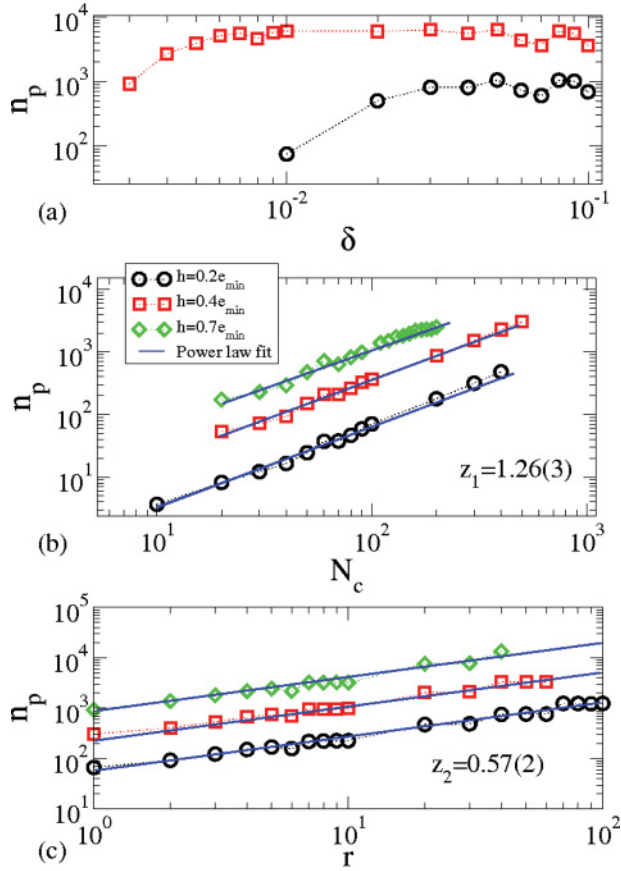
FIG. 6. (Color online) (a) Plot of n_p vs δ. (b) Plot of n_p vs N_c. A power law fitting gives that $z_1 = 1.26(3)$. The control parameters used were $r = 1$ and $\delta = 0.5$. (c) Plot of n_p vs r for the parameters $N_c = 33.18$ and $\delta = 0.5$. A power law fitting gives that $z_2 = 0.57(2)$.

FIG. 7. (Color online) (a) Plot of P vs n for different positions of the hole, namely, $h = 4$, 6, 10, and 12. The control parameters used were $N_c = 33.18$, $r = 1$, and $\delta = 0.5$. The dashed lines were obtained via an exponential fit. (b) Merger, for small n, of all curves shown in (a) after a rescaling $n \rightarrow n/h^{2.5}$.

shown in Fig. 6(a). By considering the two parameters N_c and r, we can suppose that

$$n_p \propto N_c^{z_1} r^{z_2}, \qquad (3)$$

where z_1 and z_2 are exponents. Plots of n_p for a large range of N_c and r are shown in Figs. 6(b) and 6(c), where a power law gives that $z_1 = 1.26(3)$ and $z_2 = 0.57(2)$. The plots shown in Figs. 6(b) and 6(c) make us to suppose that n_p is scaling invariant with respect to N_c and r. This means that a proper rescaling to the n axis, i.e., $n \rightarrow n/N_c^{z_1}$ for fixed r and δ, will collapse all the curves into a single curve, as shown in Fig. 4(b). A similar procedure for $n \rightarrow n/r^{z_2}$, considering fixed N_c and δ, collapses all the curves into a single one as shown in Fig. 4(c).

Let us now discuss the behavior of the survival probability, which we define as

$$P = \frac{1}{N} \sum_{j=1}^{N} N_{surv}(n), \qquad (4)$$

where the summation is taken along the ensemble of N different initial conditions and $N_{surv}(n)$ is the number of initial conditions that do not have enough energy to escape through the hole until a time n. When Eq. (4) is evaluated in a fully chaotic dynamics its behavior is an exponential [31],
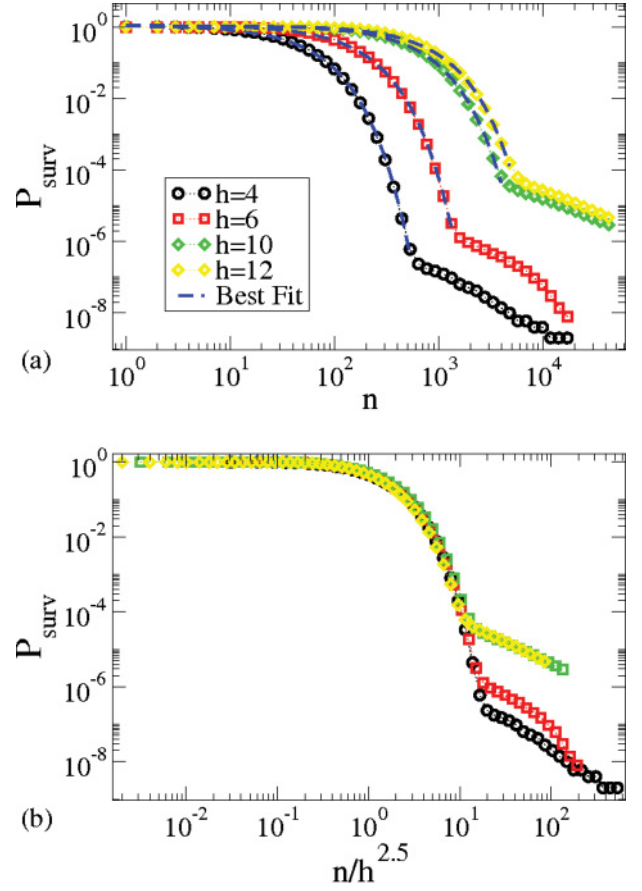
while for a mixed phase space where periodic orbits exist, the exponential decay turns into a power law [29].

We obtain the behavior of P as a function of n for different positions of the hole, as shown in Figs. 7(a) and 7(b). We see that the initial behavior, as shown in Fig. 7(a), is clearly an exponential decay $P \propto \exp(\gamma n)$, until the curve reaches a crossover n_x and changes to a slower decay, indicating the existence of sticky regions in the phase space. The slope of the exponential decay is plotted as function of the position of the hole, as shown in Fig. 8. Figure 7(b) shows a merger, for small n, of all curves plotted in Fig. 7(a) after a rescaling $n \rightarrow n/h^{2.5}$, confirming scaling invariance of the survival probability for small n. Similar overlap was observed for different combinations of control parameters as well as different initial energies.

The decay of the survival probability in Fig. 8 is almost independent of the parameter N_c. This indicates that for the range of (fixed) h shown, which is in the strongly chaotic region corresponding to $e \lesssim 0.7e_{min}$ (see Fig. 2), the transport of energy with n is apparently almost independent of N_c.

If we assume that this transport is similar to normal Brownian diffusion, we predict that the number of collisions required to diffuse on average to an energy h is proportional to h^2. For $h = 0.7e_{min}$ as in Figs. 4 and 6, this means
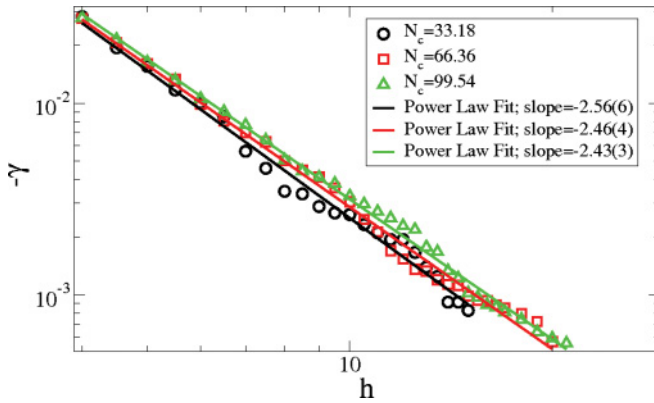
FIG. 8. (Color online) Slope of the exponential decay γ as function of h for three different values $N_c = 33.18$, 66.36, and 99.54 for $r = 1$ and $\delta = 0.5$. The straight lines are the best fits for each N_c.

we expect that n_p is proportional to e_{min}^2, which in turn is proportional to $N_c^{2\alpha_1}$ (Fig. 3). However, due to the existence of sticky regions including mainly the islands, the transport is not exactly normal Brownian diffusion. Hence, we can expect that $z_1 \leqslant 2\alpha_1$ and $z_2 \leqslant 2\alpha_2$. Such diffusive laws also predict that the distribution of escape times follows a single curve when scaled appropriately with N_c and r as shown in Fig. 4.

At longer times and when the particle reaches higher positions in the phase space where islands exist, diffusion is not Brownian. The stickiness surrounding the elliptic islands leads to slower decay as observed at the longest times in Fig. 7. Interestingly, even in the intermediate time regime, where decay is approximately exponential, there is a subtle deviation from a normal diffusive law: the exponents in Fig. 8 are significantly different from -2. Thus the stickiness

corresponding to very small elliptic islands, many of which are invisible in Fig. 2, has the effect of enhancing long time correlations, even in an apparently strongly chaotic regime.

III. SUMMARY AND CONCLUSIONS

We studied the problem of a classical particle confined inside a box of infinite potential containing a periodically oscillating square well. The transport of energy was found to be independent of the driving frequency in the low-energy, strongly chaotic regime. A histogram of escape frequency at short times was measured and characterized as invariant under a scaling consistent with normal diffusion of energy as a function of the number of collisions n. The survival probability plotted as a function of n was exponential initially and, after a crossover, followed a slower decay at late times. Both the exponential and the slower decay showed evidence of the stickiness arising from islands in the mixed phase space.

For this model we have used the escape properties with a variable hole to elucidate the dynamics at a level not visible in a phase space plot such as Fig. 2. The escape rate, which focuses on unusual trajectories at long times, exhibits features not accessible to average properties of trajectories. The anomalous dependence of an exponential escape rate with the hole parameter is of particular interest and deserves further study in more general contexts: theoretical and experimental, classical and quantum mechanical.

[1] M. Buttiker and R. Landauer, Phys. Rev. Lett. **49**, 1739 (1982).

[2] M. Leng and C. S. Lent, Phys. Rev. Lett. **71**, 137 (1993).

[3] L. P. Kouwenhoven, F. W. J. Hekking, B. J. van Wees, C. J. P. M. Harmans, C. E. Timmering, and C. T. Foxon, Phys. Rev. Lett. **65**, 361 (1990).

[4] P. S. S. Guimarães, B. J. Keay, J. P. Kaminski, S. J. Allen, Jr., P. F. Hopkins, A. C. Gossard, L. T. Florez, and J. P. Harbison, Phys. Rev. Lett. **70**, 3792 (1993).

[5] L. P. Kouwenhoven, S. Jauhar, J. Orenstein, P. L. McEuen, Y. Nagamune, J. Motohisa, and H. Sakaki, Phys. Rev. Lett. **73**, 3443 (1994).

[6] R. B. Hwang, IEEE Trans. Antennas Propag. **54**, 755 (2006).

[7] F. R. N. Koch, F. Lenz, C. Petri, F. K. Diakonos, and P. Schmelcher, Phys. Rev. E **78**, 056204 (2008).

[8] J. L. Mateos and J. V. José, Physica A **257**, 434 (1998).

[9] J. L. Mateos, Phys. Lett. A **256**, 113 (1999).

[10] O. Farago and Y. Kantor, Physica A **249**, 151 (1998).

[11] E. D. Leonel and P. V. E. McClintock, Phys. Rev. E **70**, 016214 (2004).

[12] P. K. Papachristou, F. K. Diakonos, E. Mavrommatis, and V. Constantoudis, Phys. Rev. E **64**, 016205 (2001).

[13] P. K. Papachristou, F. K. Diakonos, V. Constantoudis, P. Schmelcher, and L. Benet, Phys. Lett. A **306**, 116 (2002); Phys. Rev. E **70**, 056215 (2004).

[14] E. D. Leonel and J. K. L. Silva, Phys. A **323**, 181 (2003).

[15] G. A. Luna-Acosta, G. Orellana-Rivadeneyra, A. Mendoza-Galván, and C. Jung, Chaos Solitons Fractals **12**, 349 (2001).

[16] E. D. Leonel and P. V. E. McClintock, Chaos **15**, 033701 (2005).

[17] V. Berdichevsky and M. Gitterman, Phys. Rev. E **59**, R9 (1999); J. Phys. A **29**, L447 (1996).

[18] E. D. Leonel and P. V. E. McClintock, J. Phys. A **37**, 8949 (2004).

[19] G. M. Zaslavsky, Phys. Rep. **371**, 461 (2002).

[20] G. M. Zaslavsky, *Physics of Chaos in Hamiltonian Systems* (Imperial College Press, London, 1998).

[21] G. Cristadoro and R. Ketzmerick, Phys. Rev. Lett. **100**, 184101 (2008).

[22] C. Manchein and M. W. Beims, Chaos Solitons Fractals **39**, 2041 (2009).

[23] E. G. Altmann, E. C. da Silva, and I. L. Caldas, Chaos **14**, 975 (2004).

[24] E. G. Altmann, A. E. Motter, and H. Kantz, Phys. Rev. E **73**, 026207 (2006).

[25] L. Benet and O. Merlo, Phys. Rev. Lett. **100**, 014102 (2008).

[26] C. Simó and A. Vieiro, Nonlinearity **22**, 1191 (2009).

[27] C. Jung, O. Merlo, T. H. Seligman, and W. P. K. Zapfe, New J. Phys. **12**, 103021 (2010).

[28] C. Simó and A. Vieiro, Physica D **240**, 732 (2011).

[29] E. G. Altmann and T. Tél, Phys. Rev. E **79**, 016204 (2009).

[30] H. Buljan and V. Paar, Phys. Rev. E **63**, 066205 (2001).

[31] L. A. Bunimovich and C. P. Dettmann, Europhys. Lett. **80**, 40001 (2007).

[32] C. P. Dettmann and E. D. Leonel, e-print arXiv:1010.2228.

[33] J. A. de Oliveira, R. A. Bizão, and E. D. Leonel, Phys. Rev. E **81**, 046212 (2010).